Journal of Applied Polymer Science

Bio-inspired synthesis of molecularly imprinted nanocomposite membrane for selective recognition and separation of artemisinin

Jiuyun Cui,[1] Yilin Wu,[1] Minjia Meng,[1] Jian Lu,[2] Chen Wang,[1] Juan Zhao,[1] Yongsheng Yan[1]
[1]School of Chemistry and Chemical Engineering, Jiangsu University, Zhenjiang 212013, China
[2]School of Chemistry and Chemical Engineering, Jilin Normal University, Zhenjiang 212013, China
Correspondence to: Y. Yan (E-mail: CJY18252586640@163.com)

ABSTRACT: Inspired from the highly bioadhesive performance of mussel protein, a simple, yet efficient synthetic method for efficiently imprinting of Artemisinin (Ars) was developed to prepare the bio-inspired molecularly imprinted membranes (MIMs) via atom transfer radical polymerization (ATRP). In this work, attributed to the unique properties of polydopamine (pDA) modified layers and ATRP technology, the uniform recognition sites for efficiently selective extraction of the Ars with high stability could be obtained on the MIMs surfaces. In addition, the maximum adsorption capacity of the MIMs is 158.85 mg g^{-1} by the Langmuir isotherm model, which is remarkable higher than NIMs. Additionally, because of the formation of the uniform specific recognition cavities on membrane surfaces, the as-prepared MIMs exhibited a rapid adsorption dynamics and well-fitted for the pseudo-second-order rate equation, also, possessed an excellent per-selectivity performance ($\beta_{artemether/Ars}$ values is 0.18) of template molecule, which clearly demonstrated the potential value of this method in the selective separation and purification of Ars. © 2016 Wiley Periodicals, Inc. J. Appl. Polym. Sci. **2016**, *133*, 43405.

KEYWORDS: adsorption; membranes; molecular recognition; nanostructured polymers

Received 10 October 2015; accepted 4 January 2016
DOI: 10.1002/app.43405

INTRODUCTION

Artemisinin (Ars), the excellent Lactones drug, which is used for curing malaria, especially cerebral malaria and chloroquine resistant falciparum malaria because of its high efficiency and low toxicity.[1–4] Ars is used to interfere with the surface film of Plasmodium Falciparum, it is that to say the structure of insect is destroyed. However, now commercially available Ars mainly extracted from plants, which is rare and due to wide application, it possesses expensive price.[5,6] Traditional extraction method is a time-consuming, high-cost and multiprocess.[2,3] Therefore, with the rapid increase of market demand of Ars,[7–10] it is essential to establish an environment friendly, low cost, simple, and convenient approach, which will be effective to enrich artemisinin in future.

As one of the most promising way to separation and selective recognition of compound, molecular imprinting technique (MIT) is regarded as an attractive mimetic approach to create specific recognition cavities chemically complementary to target molecule.[11–14] The cross-linking monomer leads to formation of a three-dimensional polymer network for target molecule. Then removed the template and leaved a cavity where is capable to rebind the specific target molecular.[15–20] Nevertheless, separating the template molecular needs multiple time and complex steps by MIT but still, membrane separation technology has been extensively used in pharmaceutical production.[21] Combination of MIPs into nanoporous membranes can provide membrane-based specific separation for target molecules. Recently, molecularly imprinted membrane technology (MIMT) has got much attention and rapid development in field of separation and analysis due to combining the MIT and molecular imprinting polymers (MIPs), owning their stability, feasibility in different kinds of conditions, and without using a lengthy and costly separation stage.[22–25] However, the inherent issues of formation of heterogeneous recognition sits impact on specific selectivity and regeneration. Therefore, it is modified to control surface properties and give meaningful functionalities to membrane surface.

Atom transfer radical polymerization (ATRP)[26–30] is a far reaching for reversible deactivation and radical polymerization system to modify the interfacial properties, which is widely utilized and operated by controlled/living polymerization during the redox equilibrium process mediated with a binding metal catalyst.[31,32] Additionally, ATRP is an efficient approach via controlled radical polymerization to obtain polymeric material. In other

Additional Supporting Information may be found in the online version of this article.

words, the polymerization of various monomers was controlled molecular weight and chain architectures with low energy and high livingness.[33–36] Therefore, the method of ATRP has been more attracted due to its controlled/living radical polymerization and achieve uniform polymerization onto membrane surface.

In the present article, we have selected the polyvinylidene fluoride (PVDF) membrane as the support matrix, it has a high mechanical strength, chemical corrosion resistance and so on. PVDF membranes as one of the ideal solid phase support material in the imprinting method, deposit on membrane surface by the dopamine with its self-assembled, which accomplish in the facile atmosphere and simple process. The dopamine, will be easily attached to a variety of solid surface with strong covalent and noncovalent interactions polymerization. Next, Ars as template molecular and AM as functional monomer prepolymerize to formation of binding sites. In addition, ethylene glycol dimethacrylate (EGDMA) as cross-linking synthesis imprinted membrane by ATRP technique, coming into being uniform recognition sites on the membrane surface. It was an innovative way for selectivity separation of Ars and worked efficiently with much higher adsorption capacity for membrane. The excellent selectivity and separation ability for the Ars help us in resolving issues and obtaining Ars in short supply.

EXPERIMENTAL

Regent and Materials

PVDF powder and n-methyl pyrrolidone (NMP) were achieved from Millipore Inc. Tris (hydroxymethyl) aminomethane (Tris-HCl, 99%), dopamine (98%) were purchased from Aladdin Reagent Ethanol (P99.5%), acrylamide (AM, 98.5%), artemisinin (Ars, 98%), artemether (98%), copper(II) bromide ($CuBr_2$), 2,2'-bipyridine (98%), ethylene glycol dimethacrylate (EDGMA, 98%) were obtained from Sinopharm Chemical, Reagent (Shanghai, China). The above reagents were all analytical grade or better. Doubly distilled water was used for cleaning processes and preparing all aqueous solutions.

Instruments

X-ray photoelectron spectroscopy (XPS) was used to further investigate chemical compositions of membranes surface with an ESCALAB 250 spectrometer. The character of PVDF membrane and MIMs was observed through scanning electron microscopy (SEM, S-4800). HPLC (Agilent 1200 series, USA) was use for detecting the concentrations of Ars and artemether. The determination requirements were consisted of 1.0 mL min^{-1} flow rate, methanol/H_2O (80/20, v/v) mobilephase, 25 °C column temperature and 217 nm UV detection.

Synthesis of Pristine PVDF Membrane

Four gram PVDF powder and 21 g NMP were fully mixed in three round bottom flask, then as-prepared casting solution was sealed and mechanical stirring for 24 h at 50 °C ensure complete dissolution of solvent (NMP). In order to remove bubbles in casting solution, it was stopped to stir and let it remained stationary for 12 h at 50 °C. The obtained solution was cast to glass plate with doctor knife. Then as-prepared membrane with glass plate was immersed into deionized water to undergo a phase transformation process. After about 1 h, the pristine membranes were obtained. The membranes were peeled off from glass plate and kept in deionized water for the following used.

Synthesis of Modified PVDF Membrane by the Dopamine

By taking a piece of pristine membrane (40 mm in diameter) and dopamine (200 mg) into 100 mL 10 m*M* Tris-HCl (pH = 8.5) aqueous, and kept it for mechanical oscillation for 12 h at RT. After that, a dopamine layer deposited of PVDF membrane surface (pDA@PVDF) was achieved and rinsed by deionized water to remove the remaining organic species and kept for drying in vacuum at 50 °C.

The pDA@PVDF Membrane Is Further Modified by Bromoisobutyryl Bromide

Firstly, mixture solution A was prepared: a piece of pDA@PVDF membrane and 2mL Triehylamine (TEA) were dropped into 30 mL THF, which was fully mixed into ice water bath. Secondly, mixture solution B was prepared: 20 mL THF and 1.5 mL Bromoisobutyryl Btomide (2-BIB) was fully mixed, which was added into the A mixture solution dropwise. Before the prepolymerization reaction, the system was degassed with nitrogen for 30 min and sealing. The reaction was maintained for 2 h in ice water bath and then taken it out in the RT for 24 h. The achieved Br@pDA@PVDF membrane was rinsed by ethanol to move the unreacted organic matters and dried in vacuum at 50 °C.

Imprinting of Ars Molecule by ATRP

A piece of Br@pDA@PVDF membrane, 50 mg Ars, acrylamide (AM 100 mg) and 0.8 mL EGDMA was added into 40 mL ethanol and 20 mLdeionized water mixture solution, which were fully mixed in the three round bottom flask. Also, the system was degassed with nitrogen for 30 min. Then CuBr (64 mg) and pyridine (28 mg) were added into the mixture solution. The system reaction was sealed at 60 °C for 16 h. At last, the achieved molecular imprinting membrane (MIMs) was rinsed by water and ethanol to remove residual organic polymers and unreacted matters and dried in vacuum at 50 °C.

Before it using, the CuBr powder was purified by mixture of ethanol/acetic acid (9:1, V/V) in order to remove Cu^{2+}.

The as-prepared MIMs were extracted with mixed solvents of methanol and acetic acid (9:1, V/V) in a Soxhlet apparatus to remove the template molecular (Ars), until there was no detection of Ars by HPLC. The non-imprinted membrane (NIMs) was prepared with the same procedure of molecularly imprinted membrane (MIMs) except template molecular (Ars).

Batch Experiments

The experimental parameters involving contact time and initial concentration of Ars were performed by batch experiments. In adsorption isotherm experiments, to explore the adsorption capacity of Ars, MIMs, or NIMs was placed in ethanol solution of Ars for different concentrations 30, 50, 70, 100, 150, 200 mg L^{-1}, respectively. The solution was mechanical vibrated for 3 h at 25 °C and tested the solution of Ars by HPLC. The adsorption capacity of Ars was as follows:

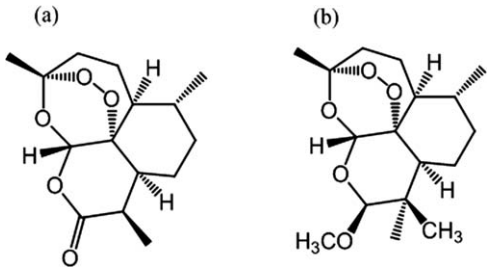

Figure 1. Chemical structures of Ars (a) and artemether (b).

$$Q_e = \frac{(C_o - C_e)V}{m} \quad (1)$$

Where Q_e (mg g^{-1}) represents the adsorption equilibrium of Ars, V (mL) and m (mg) present the volume of solution and weight of MIMs or NIMs, respectively. C_e and C_0 (mg mL^{-1}) represent equilibrium and initial concentrate of Ars, respectively.

The kinetics of adsorption as follows: MIMs or NIMs are placed in ethanol solution of Ars of 100 mg L^{-1} at 25 °C. The solution was mechanical vibrated and taken the membrane out with different time (5, 15, 30, 45, 60, 120, 180, 360 min), then tested the solution of Ars by HPLC. The Combining quantity of Ars Q_t (mg g^{-1}) was as follows:

$$Q_t = \frac{(C_0 - C_t)V}{m} \quad (2)$$

where C_t (mg mL^{-1}) is the concentration of Ars at different period of t.

Selective Permeability Tests

It is critical to the selectivity and permeability of the MIMs or NIMs due to separation and selective recognition of Ars. In the mixture solution involving analogous structure of Ars and artemether, the chemical structure of Ars and artemether are shown in Figure 1, MIMs or NIMs was placed in mixture solution of different concentrations of 30, 50, 70, 100, 150, 200 mg L^{-1}, respectively. The system was mechanically vibrated for 3 h at 25 °C and tested the solution of Ars by HPLC. The imprinting factor was as follows:

$$\alpha = \frac{Q_M}{Q_N} \quad (3)$$

Where Q_N and Q_M are the combining quantity of Ars for NIMs and MIMs, respectively.

The permeation experiments were performed by the feed solution involving 100 mg L^{-1} of Ars and artemether in ethanol. The effective area of membrane was 1.5 cm^2, which was strong fixed in the middle of the two chambers and the volume or each chamber was 150 mL. The feed solution (100 mL) of 100 mg L^{-1} was placed in one chamber, the other chamber was simultaneously placed in the same volume of ethanol. The system was mechanically oscillated, with mixture homogeneous, for 3 h at RT. The quantity of permeation mixture at different times was tested by HPLC. P ($m^2 s^{-1}$), $\beta_{\text{artemether/Ars}}$, J (mg $cm^{-1}s^{-1}$) were presented permeability coefficient, permselectivity factor, permeation flux, respectively. The obtained as follows:

$$P = \frac{J_i d}{C_{Fi} - C_{Ri}} \quad i = \text{Ars, artemether} \quad (4)$$

$$\beta_{\text{artemether}/\text{Ars}} = \frac{P_{\text{artemether}}}{P_{\text{Ars}}} \quad (5)$$

$$j_i = \frac{\Delta C_i V}{\Delta t A} \quad i = \text{Ars, artemether} \quad (6)$$

Where d represents the membrane thickness. $\Delta C_i/\Delta t$, $(C_{Fi} - C_{Ri})$ represent the change of concentration in the receiving solution, the concentration difference between feeding and receiving solutions, respectively.[37] V and A represent the volume of feeding and receiving solutions (mL), effective membrane area (cm^2), respectively.

RESULTS AND DISCUSSION

Fabrication of Prepolymerization System via ATRP

The critical for experiment is the imprinted polymerization via the surface-initiated ATRP. Functional monomer and template molecular were key role in formation of binding sites after removal of the target and obtained complementary cavities. In the procedure, to establish a uniform recognition sites by using

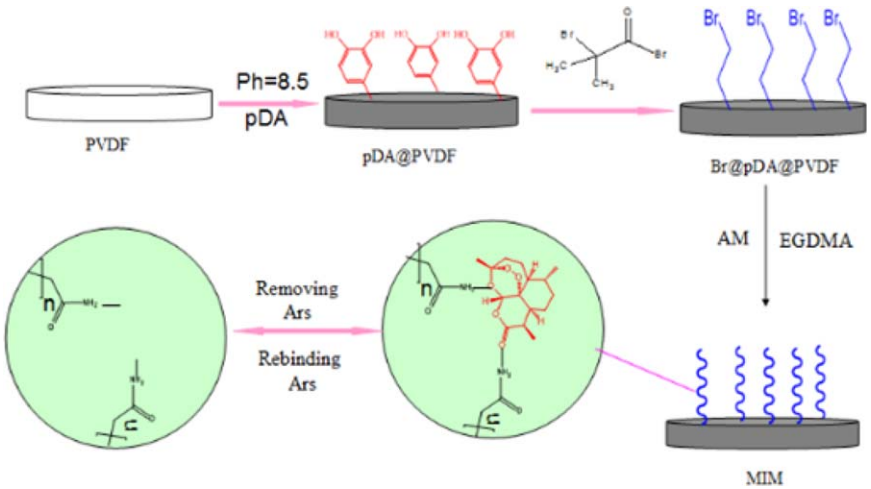

Figure 2. The synthesis process of MIMs. [Color figure can be viewed in the online issue, which is available at wileyonlinelibrary.com.]

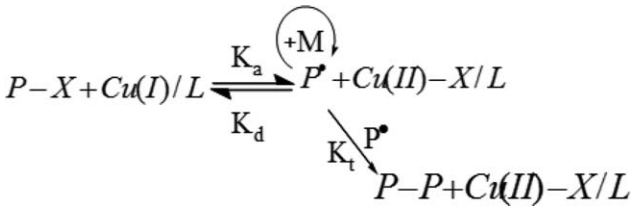

Figure 3. ATRP mechanism.

AM as the monomer and EGDMA as cross-linking. It is noted that a proper amount of the Ars added is significant for increasing the adsorption capacity, which may be indicated to increase recognition sites on the MIMs surface. An excess of Ars would have no obvious change, it is duo to the saturated binding sites on the surface of MIMs (Supporting Information S1, Figure 1). Figure 2 illustrates the synthesis mechanism of MIMs. Also, Figure 3 illustrates the ATRP mechanism. The bromine compounds as initiator induced redox equilibrium process mediating by Cu (I)-ligand catalyst. Also, the chain uniform growth relied on the reversible dormant species and active species of Cu(I)/Cu(II),-which was necessary for achieving the controlled polymerization. The surface-initiated ATRP was an important approach to graft uniform polymerization onto the surface of MIMs. In this work, the selective imprinting recognition sites of MIMs were found to be favorable to higher adsorption capacity for Ars.

In addition, X-ray photoelectron spectroscopy (XPS) was used for probing elements present of synthesized membranes.[38] The XPS wide spectra Figure 4(A) and narrow scan and Figure 4(B–D) were shown in the Figure 4. In the wide spectra Figure 4(A), comparing with the pristine PVDF Figure 4(A), the pDA@PVDF Figure 4(B) increased new peaks of N1s and O1s indicating the presence of pDA layers on the PVDF membrane. At the same time, the narrow scan for N1s Figure 4(B) and O1s Figure 4(C) also proved the existence of pDA layers. Similarly, the new emerging Br3p and Br3d peaks in wide spectra Figure 4(A) of the Br-pDA@PVDF Figure 4(C), showed that the initiator has been successfully grafted on membrane surface. Finally, as shown the wide spectra of MIMs Figure 4(D) the intensity of O1s peak enhanced, and on the narrow scan Figure 4(D), emerging new peaks of C—O—C and C═O—O of MIMs, is indicating the formation of imprinting polymerization on the surface of PVDF via ATRP.

The Figure 5 summarized the micrographs of different stages of preparing membrane used SEM with gold-sputtered samples. As shown in Figure 5, the original PVDF membrane (a-b), pDA@PVDF (c-d) and imprinting membrane(e-f) had appreciable difference in morphology. Pristine PVDF (a-b) showed a rough and porous structure turn into relative smooth and porous structure after DA self-polymerization (c-d). It is displayed that dopamine layer was coated on the surface of PVDF. In Figure 5(E,F) the decrease of pores and the obvious imprinting layers were observed from MIMs. According to the other modified membranes, different surface morphology of MIMs was indicated the imprinting polymer layer was successfully coating onto the surface of the MIMs by ATRP.

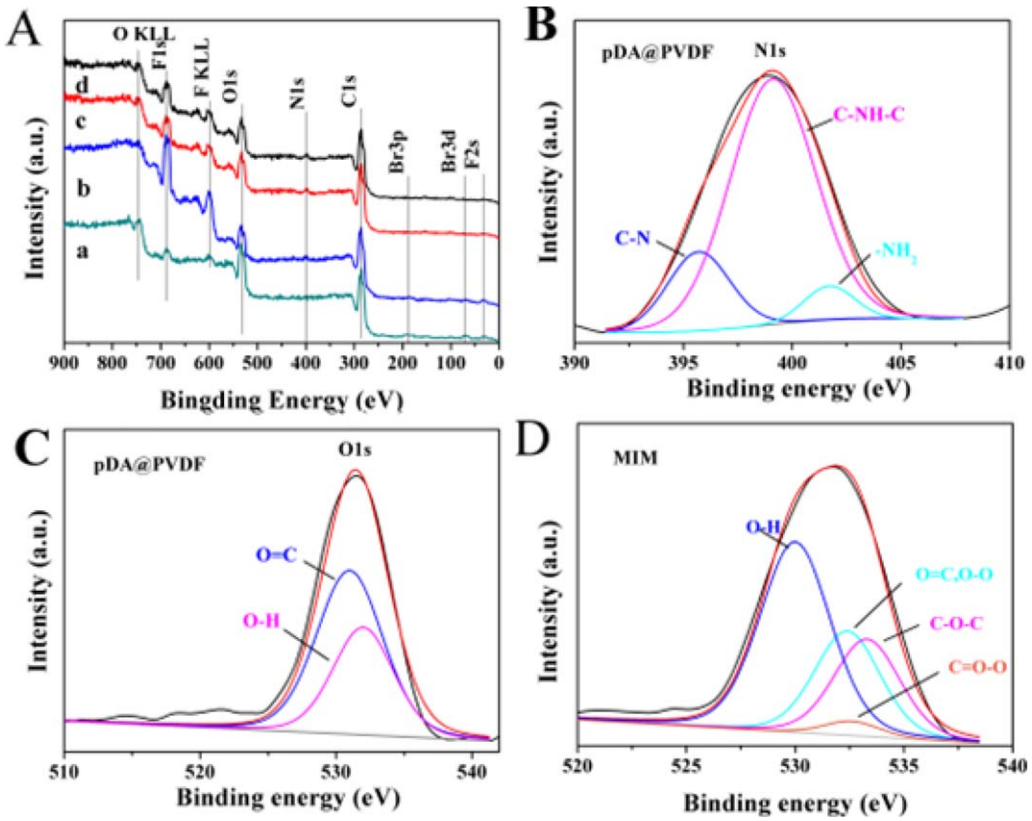

Figure 4. X-ray photoelectron spectroscopy (XPS) wide scan (A) of pristine PVDF membrane (a), pDA@PVDF (b), Br-pDA@PVDF (c) and MIMs (d), narrow scans for N1s (B) and O1s (C) of pDA, O1s (D) of MIMs. [Color figure can be viewed in the online issue, which is available at wileyonlinelibrary.com.]

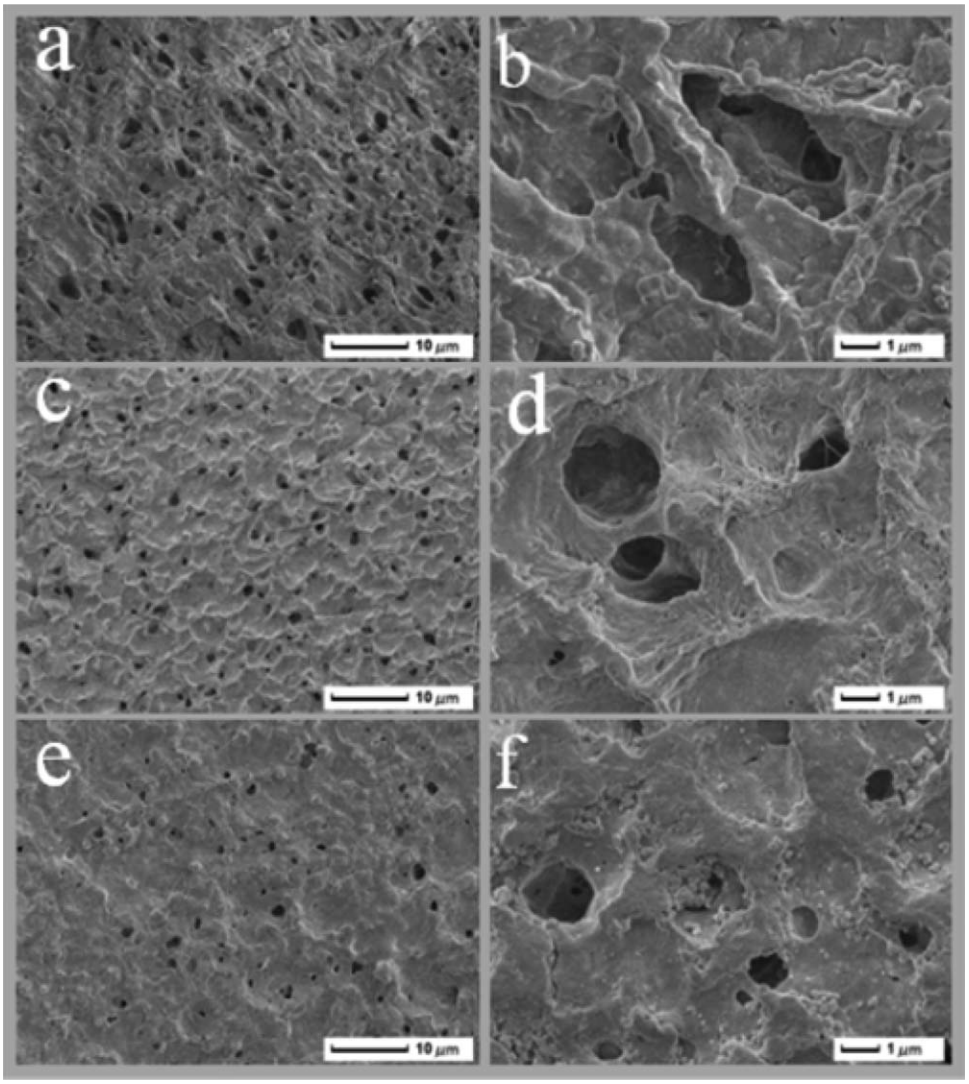

Figure 5. SEM surface images of pristine PVDF membrane (a-b), pDA@PVDF membrane (c-d) and MIMs (e-f).

Adsorption Isotherms

Equilibrium adsorption experiments were carried out to evaluate the binding text of MIMs and NIMs for Ars at 25 °C. The Figure 6 showed that the amount of Ars adsorbed on membrane with the initial different concentration from 30 to 200 mg L^{-1}. It was displayed that MIMs were apparently higher binding capacity than that of NIMs at the same condition, which suggested a great number of recognition sites and high affinity capacity for template molecular (Ars) on the surface of the MIMs. In addition, adsorption equilibrium data of MIMs and NIMs fitting to Langmuir (A) and Freundlich (B) isotherm models were shown in Figure 6. Langmuir isotherm model[39] was assumed based on monolayer adsorption, and Freundlich[40] isotherm was an empirical equation, which was presupposed adsorption behavior based on multilayer adsorption. The nonlinear expressions of the Langmuir and Freundlich modes were given by follows:

$$Q_e = \frac{K_L Q_m C_e}{1 + K_L C_e} \tag{7}$$

$$Q_e = K_F C_e^{1/n} \tag{8}$$

Where Q_m (mg g^{-1}) represents adsorption capacity of template molecules and K_L (L mg^{-1}) is the Langmuir constant, whereas K_F (mg g^{-1}) and n/1 were the Freundlich constants. Table I showed adsorption equilibrium constants and correlation coefficient (R^2). From the experimental adsorption data. The Langmuir value of R^2 was 0.9660 and the Freundlich was 0.9402, and when the value of concentration more than 150 mg L^{-1}, there is larger error in Frenudlich (B) through experimental values and theoretical values. Therefore, it was better consisted of Langmuir models. The maximum adsorption capacity of the MIMs was 158.85 mg g^{-1}, as so far, the adsorption capacity was largest as reported. Moreover, the MIMs and NIMs adsorption data was well fitted with the Langmuir model (A). In conclusion, it offered a great potential application in separation the template.

Adsorption Kinetics

The Ars adsorption kinetics curves of MIMs and NIMs were studied to investigate the binding mechanism and rate-controlling in various contact time, which was provided in Figure

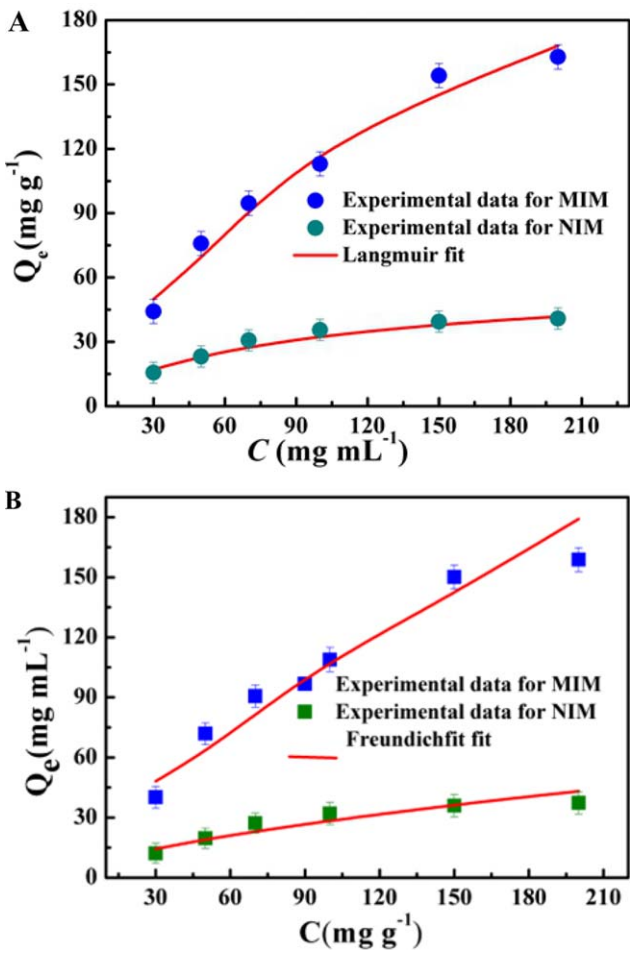

Figure 6. Equilibrium adsorption of Ars on the MIMs and NIMs, Languir model (A) and Freundlich model (B). [Color figure can be viewed in the online issue, which is available at wileyonlinelibrary.com.]

7. As shown in the Figure 7, the adsorption equilibrium of MIMs were almost achieved within 200 min. In the first 90 min, a sharp increase in the adsorption capacity owning to the presence of a large amount of effectively imprinting sites on the surface of MIMs and Ars easily reached the surface imprinting cavities of membrane. Then the slow rate that because of the recognition sites were occupied and difficult for Ars adsorption into the polymer. Following, the adsorption equilibrium of NIMs changed very small without recognition pores. Therefore, it was clearly that the specific recognition sites on the MIMs surface exhibited efficient mass transfer for template molecular.

To further understand the rate-controlling mechanism of adsorption process, the kinetic data were analyzed via the pseudo-first-

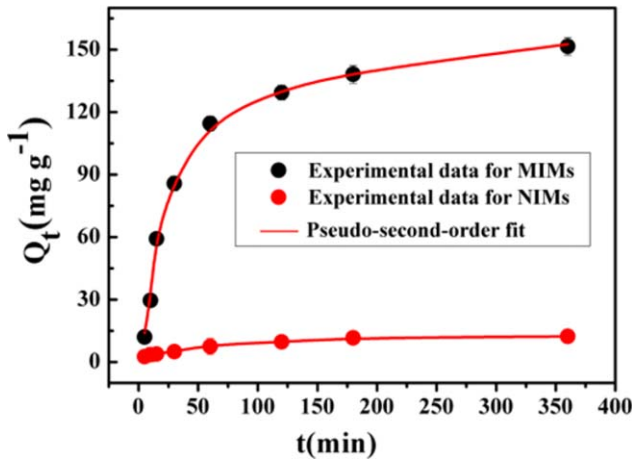

Figure 7. Adsorption kinetic curves of Ars on the MIMs and NIMs. [Color figure can be viewed in the online issue, which is available at wileyonlinelibrary.com.]

order[41] rate equation and pseudo-second-order[42] rate equation. The pseudo-first-order model is depicted as follows:

$$Q_t = Q_e - Q_e e^{-K_1 t} \tag{8}$$

The pseudo-second-order model is depicted as follows:

$$Q_t = \frac{K_2 Q_e^2 t}{1 + K_2 Q_t t} \tag{9}$$

where Q_e and Q_t (mg g^{-1}) are the amount of Ars molecules adsorbed onto adsorbent at equilibrium and time t, respectively. k_1 (min^{-1}) and k_2 is the rate constants of pseudo-first-order model and pseudo-second-order model, respectively.

The adsorption rate constants and linear values from two kinetic equations were summarized in Table II. The pseudo-second order with high regression coefficients value (R^2) provided better fit for Ars adsorption than the pseudo-first-order. Moreover, the pseudo-second-order kinetic model calculated the adsorption capacity ($Q_{e,c}$) that was close to the experimental data ($Q_{e,e}$). It was indicated that the second-order kinetic model fitted well with the kinetic adsorption data of Ars on the membrane, which suggested that the chemical process could be the rate-limiting step during the adsorption.

Selectivity Study and Recognition Mechanism

To evaluate the adsorption specificity of MIMs, the selectivity study was carried out toward Ars and its structural analogue artemether at the concentration of 100 mg L^{-1}. As shown in Figure 8, the MIMs exhibited remarkably high adsorption capacity for Ars in the presence of the similar structural compounds, illustrating that the adsorption capacity was hardly affected even when structurally similar compounds coexisted. By

Table I. Langmuir Parameter for the Adsorption of Ars onto the MIMs and NIMs

	Langmuir			Freundlich		
Adsorbent	K_L	Q_e	R^2	K_F	1/n	R^2
MIMs	0.014	158.85	0.9660	8.8560	0.6024	0.9402
NIMs	0.014	37.35	0.9636	2.3096	0.5594	0.9032

Table II. Adsorption Rate Constants of Ars Involve Pseudo-First-Order and Pseudo-Second-Order Model

	Pseudo-first-order model				Pseudo-second-order model		
Adsorbents	$Q_{e,exp}$ (mg g^{-1})	$Q_{e,cal}$ (mg g^{-1})	k_1 (min^{-1})	R^2	$Q_{e,cal}$ (mg g^{-1})	k_2 (min^{-1})	R^2
MIMs	154.55	160.08	0.0050	0.8312	156.20	0.00016	0.9914
NIMs	10.36	14.38	0.0002	0.8123	10.72	0.00065	0.9871

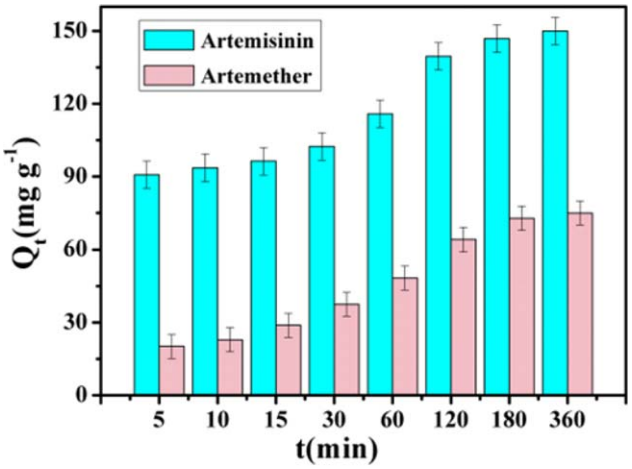

Figure 8. Adsorption selectivity of MIMs toward different targets. [Color figure can be viewed in the online issue, which is available at wileyonlinelibrary.com.]

calculation, the α value of MIMs of Ars to artemether was 2.04, which was due to these recognition sites with their own shape, sites, and functionalities complementary for target molecules. Therefore, it can be concluded that the imprinting sites on the MIMs surface had a good selectivity for Ars and the recognition ability was stemmed from imprinting sites via ATRP.

Permeation and Separation Mechanism of Ars. According to the template molecular in MIMs by different transfer mode, the selective permeation is generally divided into two mechanisms, which are facilitated permeation and retarded permeation. In this work, to evaluate the permselectivity of the MIMs and NIMs, the permeability experiment was performed involving competitive compound concentrations of Ars and Artemether of both 100 mg L^{-1}. The permselectivity curves of the mixture through different membranes were shown in Figure 9. It can be seen that the concentration of Ars in the receptor chamber was much higher than artemether through MIMs, whereas NIMs was not the case coming from the imprinting effect. The result shows imprinted sites had an affinity with Ars and it could preferentially transferred from one side to another side. It is main because that Ars in the feed solution is easily combined with recognition sites through covalent bond or semi-covalent bond. Following, the bond is destroyed by concentration gradient and transferred to MIMs another side. In the discussion, the perm-selective of Ars and its analogy structure results were according with the facilitated permeation.[21] In addition, the permselectivity performance was summarized in Table III. From the value of P and $\beta_{artemether/Ars}$, it is can be seen that MIMs have high selective recognition ability than NIMs.

Regeneration Analysis

The regeneration model of MIMs was performed by five sequential cycles of adsorption-desorption. During the desorption procedure, the mixture of methanol and acetic acid (9:1, V/V) was used 50 mL in a Soxhlet apparatus to remove the template molecular (Ars), changing mixture solution at one hour intervals until there was no detection of Ars by HPLC. In the adsorption procedure, regeneration MIMs were placed in ethanol solution of Ars of 100 mg L^{-1} which was mechanical vibrated and taken the membrane out for 3 h at 25 °C and tested the solution of Ars by HPLC. As shown in Figure 10, the rebinding capacity of MIMs was still remained steady after five regenerated cycles with only loss of 8.2% of the initial value, which might be

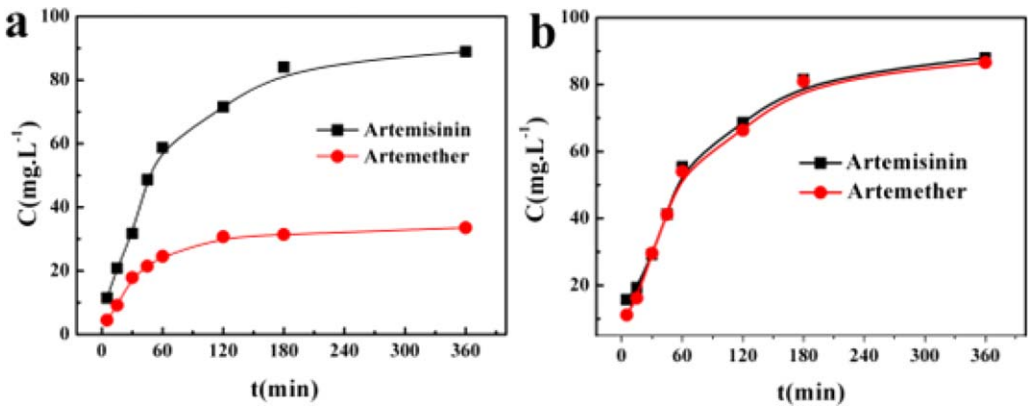

Figure 9. Permeation performances of MIMs (a) and NIMs (b) toward aeremisinin an artemether. [Color figure can be viewed in the online issue, which is available at wileyonlinelibrary.com.]

Table III. Permeation test results of MIMs,NIMs for Ars and artemether moleculaes

Membranes	Substrate	J (mg $cm^{-2}s^{-1}$)×10^{-4}	P (cm^2s^{-1})×10^{-4}	$\beta_{artemether/Ars}$
MIMs	Ars	12.5	3.67	0.81
	artemether	2.68	0.65	
NIMs	Ars	8.91	2.52	0.96
	artemether	8.57	2.43	

the reduction of a few recognition sites in polymer matrix during the cycles of regeneration process. Overall, the MIMs possessed good affinity and stability to Ars even after five times of regeneration. The result implied the MIMs reused to further selective recognition and separation for Ars for least five times.

CONCLUSIONS

In this research article, for the first time, we have proposed a bio-inspired imprinting membrane methodology using PVDF as the support material involving straightforward synthesis techniques for preparing the MIMs, which was innovatively used as a highly efficient novel system for harvesting the selective separation system of Ars molecule. The novel bioadhesive composite structure was achieved firstly by a dopamine self-polymerization process, followed by an ATRP method on the surface of PVDF membrane. Attributing to the ATRP technology uniformly dispersed and tightly bound recognition sites could be formed onto the membrane surfaces. Importantly, in comparison with the conventional approaches, the present versatile method possess both selective separation and recognition performance based on the adsorption isotherms and the maximum adsorption capacity was reached 158.85 mg g^{-1}. Additionally, the selective separation performance and permeation experiments (βvalue is 0.81) revealed that MIMs have a better selectivity and stability performance with reusing at least five times than NIMs, which due to the formed imprinting sites on the membrane surface and the rebinding capacity for Ars. It is noteworthy that this work provides a simple and convenient way, which would be valuable for further application towards Ars. As a concluding remarks, we envisage that this technique provides a low cost, yet environmental way for efficient separation and enrichment of Ars molecule.

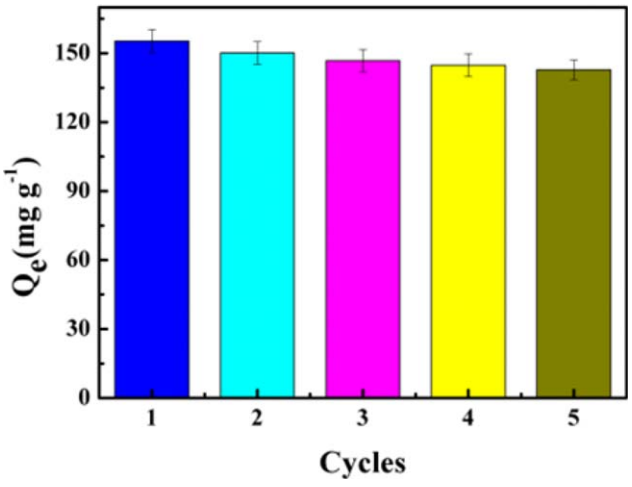

Figure 10. Adsorption stability and regeneration performances of MIMs after five times of adsorption−desorption cycles. [Color figure can be viewed in the online issue, which is available at wileyonlinelibrary.com.]

ACKNOWLEDGMENTS

This work was financially supported bythe National Natural Science Foundation of China (Nos. U1507118, U1407123, 21406085), Special Financial Grant from the China Postdoctoral Science Foundation (2014T70488), Natural Science Foundation of Jiangsu Province (BK20140580), and Ph.D. Programs Foundation of Ministry of Education of China (No. 20133227110022).

REFERENCES

1. Li, C. H.; Tai, W. K.; Sheng, P. Q.; Guo, C. X.; De, H. Z. *Electrophoresis* **2002**, *23*, 2865.
2. Kohler, M.; Haerdi, W.; Christen, P.; Veuthey, J. L. *J. Chromatogr. A* **1997**, *785*, 353.
3. Hao, J.; Han, W.; Shi, C.; Deng, X. *Sep. Purif. Technol.* **2002**, *28*, 191.
4. Hsu., E. *Trans. R. Soc. Trop. Med. Hyg.* **2006**, *100*, 505.
5. Zhang, L.; Ye, H. C.; Li, G. F. *J. Integr. Plant Biol.* **2006**, *48*, 1054.
6. Abdin, M. Z.; Israr MRehman, R. U.; Jain, S. K. *Planta Med.* **2003**, *69*, 289.
7. Maier, N. M.; Lindner, W. *Anal. Bioanal. Chem.* **2007**, *389*, 377.
8. Yano, K.; Karube, I. *TrAC, Trends. Anal. Chem.* **1999**, *18*, 199.
9. Piletska, E. V.; Karim, K.; Cutler, M.; Piletsky, S. A. *J. Sep. Sci.* **2013**, *36*, 400.
10. Visnjevski, A.; Schomäcker, R.; Yilmaz, E.; Brüggemann, O. *Catal. Commun.* **2005**, *6*, 601.
11. Xie, C.; Li, H.; Li, S.; Wu, J.; Zhang, Z. *Anal. Chem.* **2010**, *82*, 241.
12. Díaz-Díaz, G.; Diñeiro, Y.; Menéndez, M. I.; Blanco-López, M. C.; Lobo-Castañón, M. J.; Miranda-Ordieres, A. J.; Tuñón-Blanco, P. *Polym.* **2011**, *52*, 2468.
13. Huang, B. Y.; Chen, Y. C.; Wang, G. R.; Liu, C. Y. *J. Chromatogr. A* **2011**, *1218*, 849.
14. Larsen, A. T.; Lai, T.; Polic, V.; Auclair, K. *Green Chem.* **2012**, *8*, 2206.
15. Feng, T.; Sun, D.; Gao, J.; Qian, Z.; Wang, X.; Fei, T; Xie, Q. J. C. *J. Hazard. Mater.* **2013**, *244*, 750.

16. Ban, L.; Zhao, L.; Deng, B. L.; Huang, Y. P.; Liu, Z. S. *Anal. Bioanal. Chem.* **2013**, *405*, 2245.
17. Shaikh, H.; Memon, N.; Khan, H.; Bhanger, M. I.; Nizamani, S. M. *J. Chromatogr. A* **2012**, *1247*, 125.
18. Meenakshi, S.; Abhishek, K.; Nazia, T. *Anal. Bioanal. Chem.* **2013**, *405*, 4245.
19. Zian, L.; Fan, Y.; Xiwen, H.; Xiaomiao, Z.; Yukui, Z. *J. Chromatogr. A* **2009**, *1216*, 8612.
20. Wei, Z.; He, X. W.; Yang, C.; Li, W. Y.; Zhang, Y. K. *Biosens. Bioelectron.* **2012**, *31*, 84.
21. Ulbricht, M. *J. Chromatogr. B* **2004**, *804*, 113.
22. Yilin, W.; Ming, Y.; Yongsheng, Y.; Xinlin, L.; Minjia, M.; Peng, L.; Jianming, P.; Pengwei, H.; Chunxiang, L. *Langmuir* **2014**, *30*, 14789.
23. Székely, G.; Valtcheva, I. B.; Kim, J. F.; Livingston, A. G. *React. Funct. Polym.* **2015**, *86*, 215.
24. Moein, M. M.; El-Beqqali, A.; Javanbakht, M.; Karimi, M.; Akbari-Adergani, B.; Abdel-Rehim, M. *J. Chromatogr. A* **2014**, *1372*, 55.
25. Wu, Y. T.; Zhang, Y. H.; Zhang, M.; Liu, F.; Wan, Y. C.; Huang, Z.; Ye, L.; Zhou, Q.; Shi, Y.; Lu, B. *Food Chem.* **2014**, *164*, 527.
26. Wang, J. S.; Matyjaszewski, K. *J. Am. Chem. Soc.* **1995**, *117*, 5614.
27. Kato, M.; Kamigaito, M.; Sawamoto, M.; Higashimura, T. *Macromolecules* **1995**, *28*, 1721.
28. Patten, T. E.; Matyjaszewski, K. *Science* **1996**, *272*, 866.
29. Matyjaszewski, K.; Xia, J. *Chem. Rev.* **2001**, *101*, 2921.
30. Krzysztof, M.; Tsarevsky, N. V. *J. Am. Chem. Soc.* **2014**, *136*, 6513.
31. Wei, T.; Tsarevsky, N. V.; Krzysztof, M. *J. Am. Chem. Soc.* **2006**, *128*, 1598.
32. Wei, T.; Yungwan, K.; Wade, B.; Tsarevsky, N. V.; Coote, M. L.; Krzysztof, M. *J. Am. Chem. Soc.* **2008**, *130*, 10702.
33. Hansson, S.; Östmark, E.; Carlmark, A.; Malmströ, M. E. *ACS Appl. Mater. Interfaces* **2009**, *1*, 2651.
34. Carlmark, A.; Malmström, E. *J. Am. Chem. Soc.* **2002**, *124*, 900.
35. Li, C. Y.; Xu, F. J.; Yang, W. T. *Langmuir* **2012**, *29*, 1541.
36. Stmark, O.; Harrisson, E.; Wooley, S.; Malmströ, K. L. *Biomacromolecules* **2007**, *8*, 1138.
37. Wu, Y. L.; Meng, M. J.; Liu, X. L.; Li, C. X.; Zhang, M.; Ji, Y. J.; Sun, F. Q.; He, Z. H.; Yan, Y. S. *Sep. Purif. Technol.* **2014**, *131*, 117.
38. Briggs, D.; Seah, M. P. Practical Surface Analysis, 2nd ed.; Wiley: Chichester, U.K., **1999**; Vol. *I*.
39. Langmuir, I. *J. Am. Chem. Soc.* **1918**, *40*.
40. LeVan, M. D.; Vermeulen, T. *J. Phys. Chem.* **1981**, *85*, 3247.
41. Ho, Y. S.; McKay, G. *Water Res.* **1999**, *33*, 578.
42. Ho, Y. S.; McKay, G. *Process Biochem.* **1999**, *34*, 451.